

VariPath: A Database for Modelling the Variance of Human Pathways in Manual and HRC Processes with Heavy-Duty Robots

Mohamad Bdiwi*, Ann-Kathrin Harsch, Paul Reindel, Matthias Putz
Fraunhofer Institute for Machine Tools and Forming Technology IWU, Chemnitz

Abstract— Unlike robots, humans do not have constant movements. Their pathways are individually changeable and influenced by circumstances. This paper presents a method to investigate human pathway variations in a real study. In systematically selected tasks, human pathways are examined for 100 participants in manual and human-robot collaboration (HRC) scenarios. As a result, the variations of pathways are presented depending on various features: e.g. in nearly all cases the variance of women's walking pathways is smaller than that of men. VariPath database can be used in any planning process of manual or HRC scenarios to ensure safety and efficiency.

I. INTRODUCTION

Human-robot-collaboration (HRC) as a man-machine system increases the flexibility and efficiency, particularly in complex or time consuming industrial tasks [1], [2]. In addition, heavy-duty collaborative robots improve ergonomic and physically stressful tasks at all interaction levels which are mentioned in [3] and [4]. However, working together with a high payload robot can include a serious risk for humans because of the large workspace and high potential forces of the robot. According to safety requirements, the calculation of safety distances is usually based on the worst-case scenario in which the human walks straight to the source of danger. Safety distances are related to the robot's and human's velocities and assumed to be fixed values – which do not correspond to the reality. Therefore, industrial HRC processes with heavy-duty robots can rarely be designed efficiently, even at the lowest interaction level (fenceless shared workspace, without shared tasks). If the real human movements, and in particular the variance of pathways, can be described as a function of the human tasks and environmental conditions, the HRC processes can be made equally safe and efficient.

Processes in HRC can be controlled and secured in many ways. In addition to visual monitoring of the process [3], another innovative concept comprises the control of HRC processes via brainwaves [5]. These approaches secure the online process. During planning and conception of HRC-processes, verified offline information, procedures and methods must be available. Empirical studies in the HRC context often deal with human acceptance, wellbeing and user-friendliness of new technologies [6], [7]. Some further

studies also has investigated the human movement behavior created a dataset for human detection [8], [9] and [10]. However, none of them has considered the requirements for modelling the variance of human movements in the industrial sectors. In [11], a comparison for the human reactions against a moving robot and a moving human is presented. Inter alia, the human walking behavior in HRC was determined in [12] and [13]. Here, Bardot et al. defined different tasks with a large-scale robot and determined the walking velocity and the distance of the human to the TCP (Tool Center Point) or the robot base. However, in the most mentioned works the human individuality still has no real influence on the robot path planning and robot control, as is shown in Fig.1.

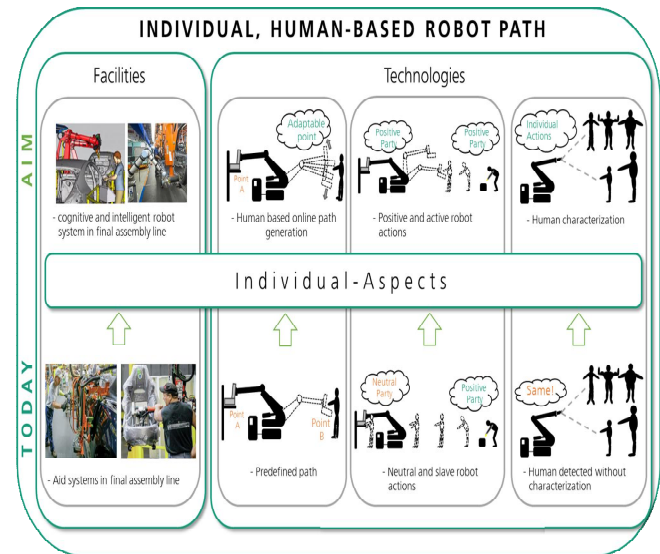


Fig. 1 Advantages of the proposed work in comparison to the state of the art.

The aim of this work to get efficient HRC scenarios without any lacks in the safety requirement. This efficient HRC-planning should take into account different requirements and properties; e.g. human anthropology, human tasks, robot tasks and environmental conditions (as shown in “individual planning conditions” in Fig. 2). A primitive approach to consider and investigate the variance of human motion behavior and walking pathways in the planning process of industrial heavy payload HRC applications is proposed in [14]. Based on that approach, this paper presents extensive investigations as an important database for modeling the human pathways. The first step is to collect a large amount of data, which covers a wide spectrum of industrial tasks and body dimensions combined

This project has been funded by the European Union (EU) and the European Fund for Regional Development (EFRE).

* Mohamad Bdiwi is the head of robotics department within Fraunhofer Institute for machine tools and forming technologies “IWU”, Chemnitz, Germany (phone: 0049 371 5397-1658; e-mail: Mohamad.bdiwi@iwu.fraunhofer.de).

with individual human movement and behavior. A systematic HRC planning process has been considered with new boundary conditions in the HRC-tasks. Based on these conditions an empirical study has been performed. The collected dataset could be the main core for new robot planning tools in HRC scenarios. Furthermore, it can be used for safe robot path planning.

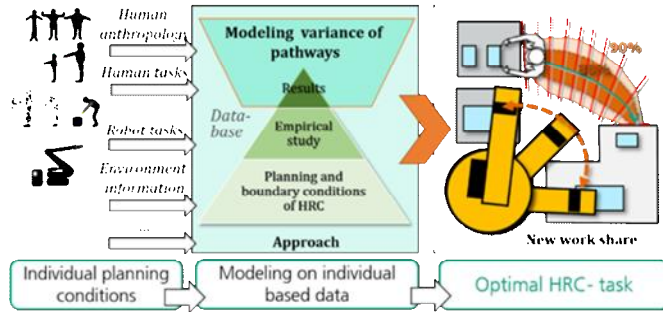


Fig. 2 Databased planning process in heavy-duty HRC, due to moving robots and individual human behavior.

II. INVESTIGATED CONDITIONS AND PARAMETERS

A. Investigation strategy

To provide a reliable database representing the variance of human motion behavior in industry, it is necessary to select experimental conditions that correspond to real production conditions.

As a first step, typical manual manufacturing activities were analyzed and listed in various industries (automotive, agriculture, etc.). It turned out that “walking” as well as “picking and placing” are the most frequently performed activities in assembly workspaces. Since “walking” occupies the larger space and holds the greater danger potential due to an increased collision risk with the robot, it was investigated in this paper.

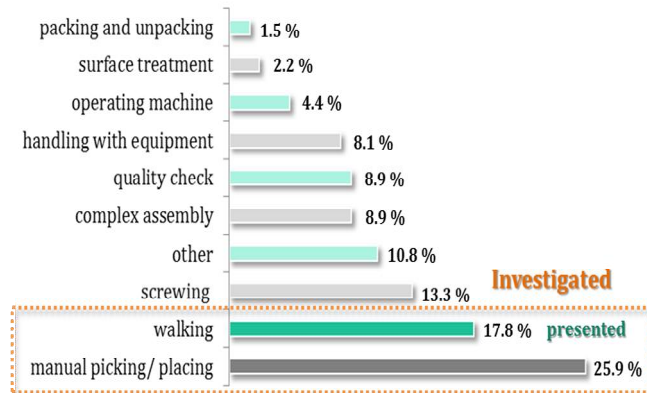


Fig. 3 Most frequent tasks in the industrial sectors.

Despite the general definition of the task, there is a large number of possible influencing variables. Thus it is possible to differentiate how long the pathway is or whether the human has to fulfill a task or not. In addition, the human can be distracted while walking or fulfilling tasks (such as carrying an object).

Fig. 4 illustrates the relevant specifications examined in the study. A reasonable combination of the tested specifications results in 16 different boundary conditions for “walking”.

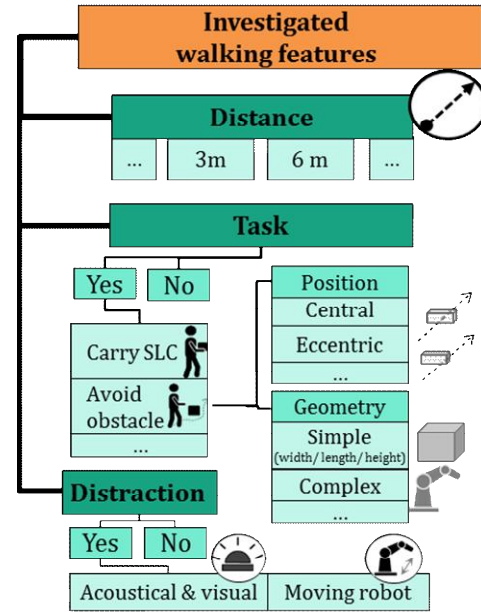


Fig. 4 Specified investigated variables.

B. Specific tested scenarios

Fig. 5 shows the layouts of the four test scenarios. The robot stage is related to the number of the scenarios.

Scenario 1 investigated the avoidance strategy of the participants (preferred side of walking along the obstacle) and the variance while passing the obstacle. A 6 m long path included a central obstacle (trolley, dimensions: 780/ 430/ 560 mm). At the starting point a SLC (Small Load Carrier, dimensions: 300 x 200 x 150 mm) of 10 kg had to be gripped at a height of 900 mm. The participant had to go from start to end point and avoid the obstacle on a freely selectable side. In each of four rounds the participant had to walk forth and back four times. After each round, the obstacle was shifted by 100 mm in the preferred walking direction without being noticed by the participant.

Scenario 2 determined the variance in pathways during a surprisingly occurring distraction. The participant had to walk 3 and 6 m in each pass, which consisted of four walks back and forth, respectively. A SLC of 10 kg also had to be randomly picked up and carried while walking. In some cases (randomized and without prior-warning of the participant) the distraction was activated in the form of a signal lamp with a siren.

Scenario 3 served to investigate the pathways when bypassing a robot over a path length of 6 m. Depending on scenario 1, the starting point was chosen so that the participant had to avoid the robot on his preferred side. The robot arm with a standard industrial gripper pointed in the direction of the walking path at a height of approx. 1.40 m and with a constant eccentricity of the robot arm of 1.15 m. The participant had to bypass the stationary robot as an

obstacle and randomly pick up and carry a 10 kg SLC for half of the passes.

In scenario 4 the test person had to walk a straight distance of 3 and 6 m while the robot was moving, providing a diffuse distraction. A SLC of 10 kg also had to be randomly picked up for half of the runs. In total, 96 curves were recorded per participant in all presented walking scenarios.

of the participants are varying extremely, e.g. body-height ranges between 1600mm until almost 2000mm and body-weight ranges from 45kg to 120kg. All this diversities make the collected measurements an optimal database for modelling the variance of the human movements in relation to their body anthropometry.

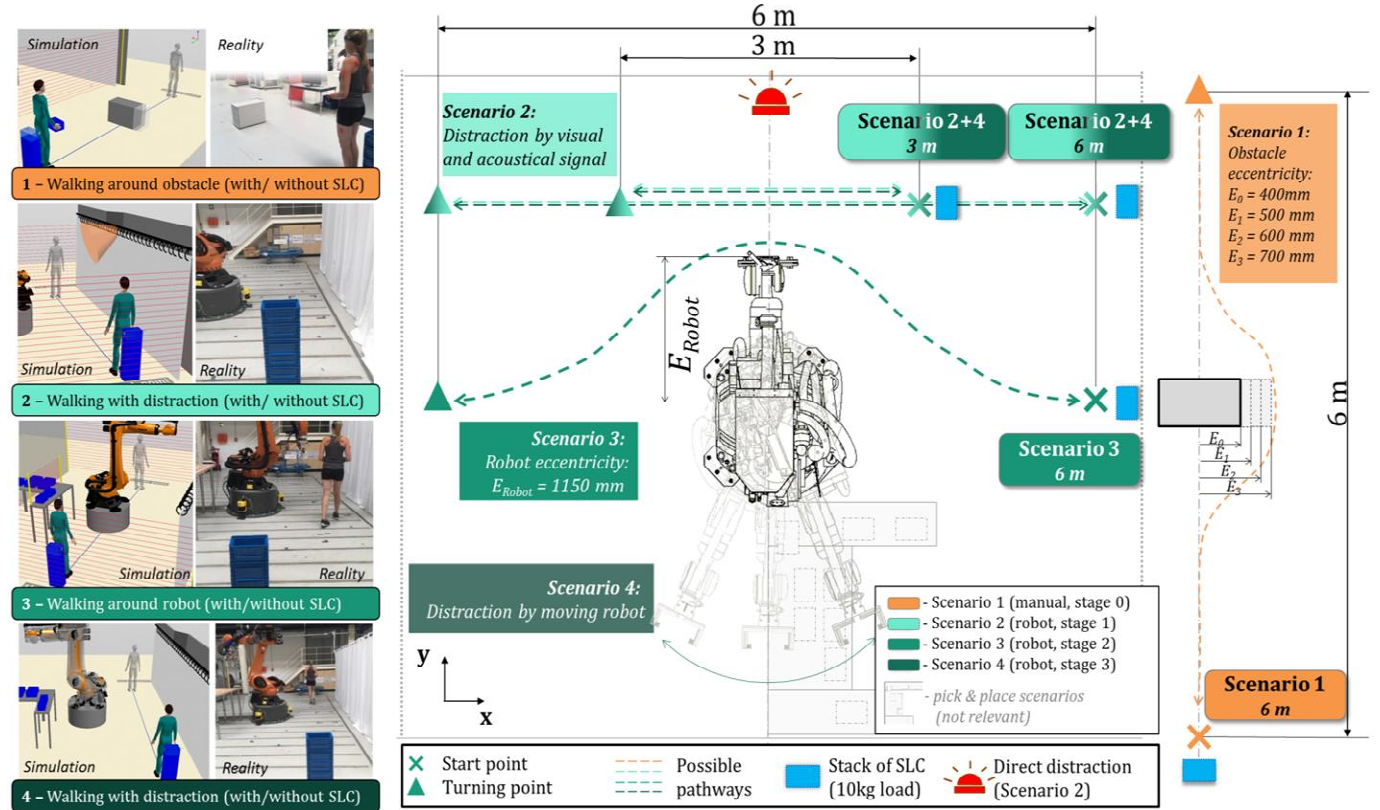


Fig. 5 Test layout to evaluate the pathways.

- Scenario 1:** robot stage 0, no robot in sight, or space for human movement available
Scenario 2: robot stage 1, stationary robot within sight, but not in space for human movement
Scenario 3: robot stage 2, stationary robot as an obstacle in space for human movement
Scenario 4: robot stage 3, moving robot within sight, but not in space for human movement

III. PARTICIPANTS AND MOTION CAPTURE SYSTEM

A. Participants

Table 1 shows the composition of the 100 examined participants. The first 10 test persons were evaluated as part of preliminary investigations to insure the accuracy of all required measurement setups. Before the evaluation and using acquired data in the modelling, the plausibility of the measurement for the rest participants have been again tested. Due to technical defects or missing data, about 20 measurement series could not be used in the final evaluation. Hence, the evaluated data differs only marginally from the total recorded data set.

As is shown in Table 1, about 65% from the evaluated measurement have been performed on men with age average between twenty and sixty-five years old, while the age structure of the female-participants ranges between eighteen and fifty years old. As is also shown, the body anthropometry

Table 1
Composition of the participant sample.

Excluded Data <i>(preliminary, missing, faulty)</i>					Evaluated					
10	3	17	70							
Male		Total recorded = 100	Number: 63				Number: 44			
	Mean		SD	Min	Max	Mean	SD	Min	Max	
Age [years]	34.3		14.7	20.0	66.0	34.0	14.9	20.0	65.0	
Body height [mm]	1820		68	1650	1980	1818	73	1650	1980	
Body weight [kg]	80.2		13.0	61.0	120.0	78.0	10.8	62.0	120.0	
Arm-span [mm]	1829		81	1590	2020	1827	87	1590	2020	
Female			Total recorded = 100	Number: 37				Number: 26		
	Mean	SD		Min	Max	Mean	SD	Min	Max	
Age [years]	26.1	7.0		18.0	50.0	27.0	8.0	18.0	50.0	
Body height [mm]	1663	60		1500	1820	1666	52	1600	1820	
Body weight [kg]	66.0	15.8		45.0	115.0	66.4	15.0	45.0	115.0	
Arm-span [mm]	1649	63		1500	1840	1651	64	1540	1840	

B. Motion capture system

The human motion data was recorded with an inertial motion capture system (XSENS Awinda®) using 17 sensors attached to body parts (Fig. 6). Accelerometers, rate gyroscopes and magnetometers are included in the inertial measurement units (IMUs) enabling the determination of acceleration, velocity and position. Using algorithms and a generated 3D human model, human movements can be reproduced.

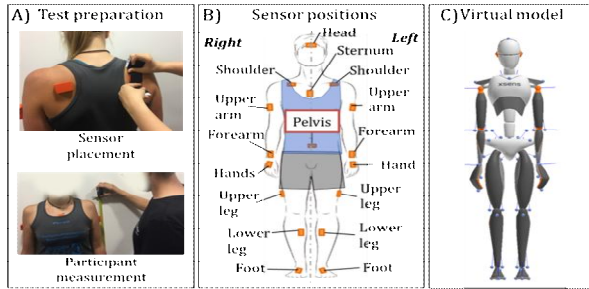


Fig. 6. Applying the Inertial Measurement Units (IMUs) to specific anatomical landmarks and the generated virtual 3D human model of Xsens®

Compared to an optical system, this system is not affected by occlusion. However, it is influenced by the magnetic field. It causes a drift of the measured values and has to be taken into account.

C. Preparation of the participants

All participants were equipped with sensors as shown in Fig. 5. The 17 sensors were attached with a skin-friendly tape to given anatomical landmarks. Next, the anthropometric data of the test persons were measured and implemented into the recording software (MVN Analyze®), creating a virtual 3D human model.

IV. DETERMINING THE VARIANCE IN PATHWAYS

A. Data evaluation

The data of the pelvis sensor (Fig. 6 B) was used to evaluate the pathways. Unlike the center of mass, which changes rapidly with the human posture, the position data of this specific sensor is more constant. Due to the magnetic field prevailing in the test field, the measured values hold a translational and/ or rotational drift. In Fig. 7 a) the recorded black curve demonstrates the drift for the path-ways of scenario 1: it does not start at the defined starting point $[x=0, y=0]$ and theoretically runs through the obstacle.

Fig. 7 a) and b) show the first steps of post processing for scenario 1, exemplarily for test person 13. Participant 13 was a woman with a height of the 95th percentile. This (randomly) means that at least 95% of German women are smaller.

The data in Fig. 7 a) was corrected in the following steps to obtain the drift-adjusted red curve and to split up the continuous black curve in individual forward and backward paths: 1. shifting the actual starting point of the black curve

to the defined start point at $[x=0, y=0]$; 2. rotating the black curve over a linear fit to the axis of the end point $[x=0]$; 3. filtering the continuous black curve over a moving average; 4. determining the turning points (as start and end points of the single curves) over the local minima and maxima (in y -direction) to split up the continuous curve into single curves (per path). All steps were repeated for each single curve. Thus, the resulted red curve had correct start-points and the end-points were just on the right axis.

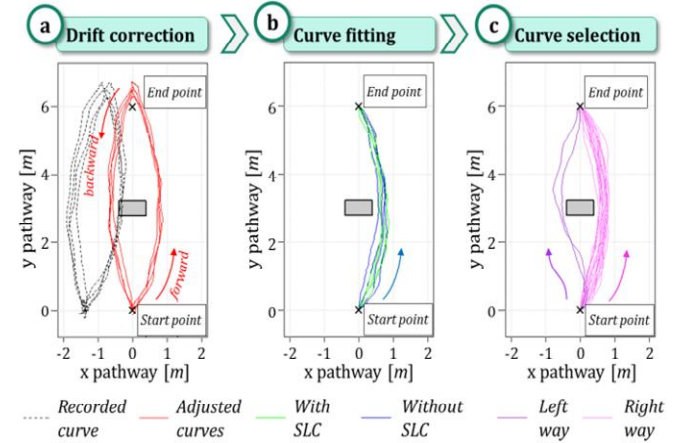


Fig. 7. Method of data recording and post processing of the pathways for each participant. Shown example: scenario 1, central obstacle (E0, with/ without SLC). a) and b) Participant 13: female, P95 body height. (8 pathways) c) All females of P95 body height, without SLC. (20 pathways)

Fig. 7 b) shows the second step, the curve fitting. Since a continuous pathway was recorded under different conditions (e.g. “with SLC”/ “without SLC”), it was not immediately possible to compare paths with the same conditions. In addition, the starting point of the backward path was the endpoint of the forward path and vice versa. So the single curves of the backward paths were shifted to the same starting point of the forward paths, were rotated by 180° towards the y -axis and fitted exactly to the end point $[x=0, y=6]$. Furthermore, the test conditions were assigned to the individual curves. In the third step all curves with same test conditions were selected. Fig. 7 c) illustrates, for example, the results for all female participants of the 95th height percentile who walked around the obstacle without a SLC.

B. Calculation of the percentiles

To compare different variables, e.g. gender or test conditions, curves recorded under the same variables were grouped. Fig.8 shows the steps to compare the distributions of the pathways of all females, who walked with and without SLC in scenario 1. Fig.8 d) shows the curves of all females without carrying a SLC. Fig.8 e) depicts the calculated percentiles for discrete points. The range between the 2.5th and 97.5th percentiles represent 95% of the measured values and is pictured with the turquoise curve. The dark green curve includes 80% of the measured values. Fig.8 f) shows the comparison of the percentiles of all females with and without SLC: Carrying an object does not seem to have a clear influence.

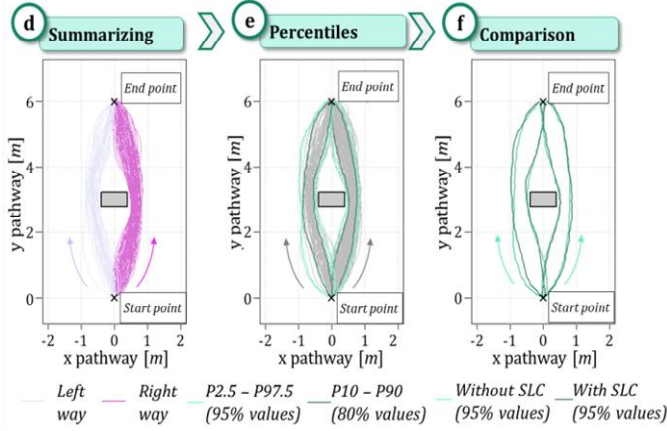


Fig. 8. Data post processing for comparing the variance in pathways for the different test conditions. d) to f) All females. (104/ 208 pathways)

C. Comparison of percentile curves

The procedure described above for drift correction, data preparation and determination of percentiles was applied to all data of the four scenarios. The curves in all scenarios were always differentiated regarding gender (“male”/ “female”), body height (“percentile 5”/ “50”/ “95” according to DIN 33402) and weight (“with”/ “without SLC”). In addition, the following parameters were considered in the scenarios: In scenario 1 a distinction was made between the eccentricity (“E0” - “E3”) and the avoidance strategy (“right”/ “left”). In scenario 2 the influencing factor “with”/ “without distraction” was evaluated. In dependence of the preferred bypassing direction scenario 3 results in an avoidance strategy of “right”/“left”. Scenario 4 comprised a constant “diffuse distraction” by the moving robot.

Fig. 9 presents an example of the results for scenario 3. It illustrates all curves including the percentiles of the male participants who bypassed the robot on the “right” side with and without SLC. It was found that the width of the percentiles, which are depicted here as scatter or variance, is smaller without carrying a SLC for all illustrated cases for males in scenario 3. Furthermore, the variance in the first half of the pathways is smaller compared to the variance when the robot was passed.

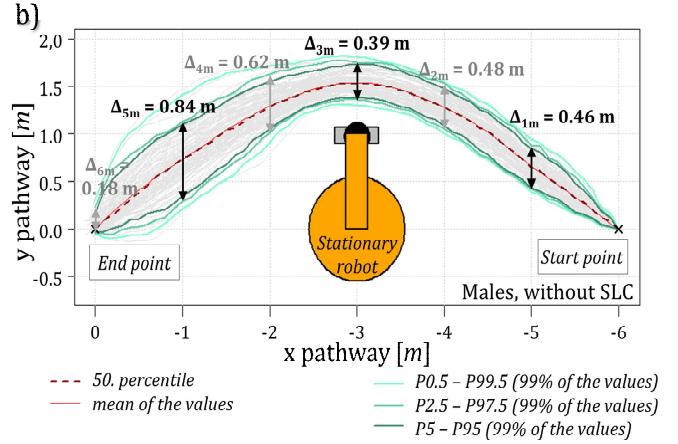
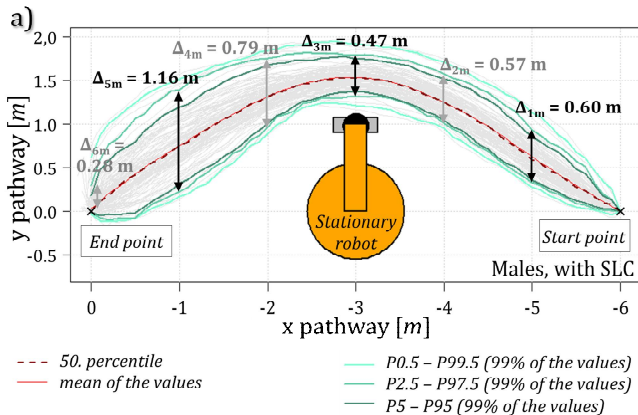


Fig. 9. Percentiles and variance of the pathway curves in scenario 3 for all males who walked around the robot on the right side. a) with SLC, b) without SLC.

The variances of the four tested scenarios and test conditions were compared by using the variances $\Delta 1m$, $\Delta 3m$ and $\Delta 5m$ (Fig. 9). It was found that 85% of the participants chose the right side when bypassing the obstacle in scenario 1. Therefore **Fehler! Verweisquelle konnte nicht gefunden werden.** presents the variance values of the specific scenarios for the “right” avoidance strategy and a distance of “6 m”.

Table 2 Variance of 95% of the recorded pathways, calculated over the delta of the 2.5th and 97.5th percentile ($\Delta 95\%, 1m$, $\Delta 95\%, 3m$, $\Delta 95\%, 5m$). Conditions: distance “6 m”, *bypassing direction (avoidance strategy) “right”

		Scenario 1*		Scenario 2		Scenario 3*		Scenario 4		
		Central obstacle		No distraction		E _{Robot}		Diffuse distraction		
		SLC	No SLC	SLC	No SLC	SLC	No SLC	SLC	No SLC	
Male	P50	Δ_{5m}	0.51	0.45	0.46	0.35	0.57	0.46	0.50	0.54
		Δ_{3m}								
		Δ_{1m}								
	P95	Δ_{5m}	0.52	0.52	0.35	0.37	0.38	0.36	0.40	0.41
		Δ_{3m}								
		Δ_{1m}								
	All	Δ_{5m}	0.57	0.56	0.44	0.37	0.47	0.39	0.45	0.53
		Δ_{3m}								
		Δ_{1m}								
Female	P50	Δ_{5m}	0.37	0.29	0.24	0.24	0.29	0.33	0.29	0.37
		Δ_{3m}								
		Δ_{1m}								
	P95	Δ_{5m}	0.29	0.26	0.36	0.45	0.31	0.32	0.20	0.45
		Δ_{3m}								
		Δ_{1m}								
	All	Δ_{5m}	0.34	0.30	0.37	0.29	0.32	0.33	0.29	0.40
		Δ_{3m}								
		Δ_{1m}								

Based on Table 2 the following valuable findings can be concluded:

1. Gender seems to have the most influence: in nearly all

tested scenarios females exhibited a smaller variance in path-ways compared to males.

2. The robot as an obstacle has a distinct influence: $\Delta 3\text{m}$ as the variance in the middle of the pathway was smaller than $\Delta 1\text{m}$ and $\Delta 5\text{m}$ in all cases of scenario 3.

3. Carrying a SLC has an ambiguous influence: the variance in pathways was rather greater when carrying an object, but this did not apply to scenario 4 and females in scenario 3.

4. The diffuse direction by a moving robot seems to have no influence: the variances of scenario 4 are rather small compared to scenario 2, but they did not differ clearly.

V. CONCLUSION

Human movements in different HRC-scenarios were systematically analyzed with a motion capture system during an extensive study. With more than 1800 measurements and 9300 walking paths a huge database for human pathways was generated for industrial applications. Post processing and evaluation of the data show that women exhibited a smaller width in the walking variance than men. When an obstacle, in particular a robot, was bypassed, the variance at the bypass point was the smallest. Finally, carrying an object had a different influence on the variance.

Taking into account the variance of human movements in planning of HRC guarantees the natural moving behavior of humans. Furthermore, the robot trajectory can be planned avoiding collisions, e.g. by using the $\Delta 95\%$ as the probable human movement space. In addition, the robot trajectory can be generated online considering the individual human profile and required tasks as is presented in Fig. 10.

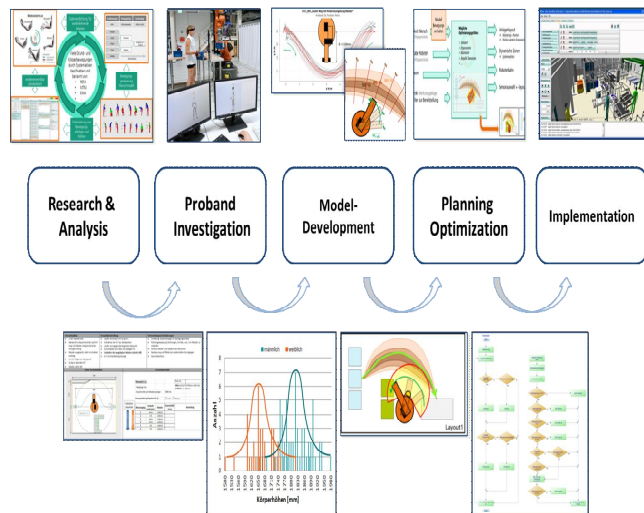


Fig. 10. Future work based on VariPath database

The collected dataset can be easily upgraded by investigation other scenarios. In other words, the influence of other variables on the human pathways and behavior in the industrial sectors could be defined and modelled. One Interesting scenario is by modelling the pathway variance and

human behavior during the work in a shared workspace with various mobile agents.

REFERENCES

- [1] Colledani, M., Gyulai, D., Monostori, L., Urgo, M., Unglert, J., van Houten, F., 2016. Design and management of reconfigurable assembly lines in the automotive industry. *CIRP Annals* 65 (1), 441–446.
- [2] Delang, K., Todtermuschke, M., Bdiwi, M., Putz, M., 2018. An approach of service modeling for the demand-driven implementation of Human-Robot-Interaction in manufacturing, in: 2018 IEEE 14th International Conference on Automation Science and Engineering (CASE). 2018 IEEE 14th International Conference on Automation Science and Engineering (CASE), Munich, Germany. 20.08.2018 - 24.08.2018. IEEE, pp. 705–710.
- [3] Bdiwi, M., Pfeifer, M., Sterzing, A., 2017. A new strategy for ensuring human safety during various levels of interaction with industrial robots. *CIRP Annals* 66 (1), 453–456.
- [4] Aaltonen, I., Salmi, T., Marstio, I., 2018. Refining levels of collaboration to support the design and evaluation of human-robot interaction in the manufacturing industry. *CIRP Annals* 72 (2018), 93–98.
- [5] Mohammed, A., Wang, L., 2018. Brainwaves driven human-robot collaborative assembly. *CIRP Annals* 67 (1), 13–16.
- [6] Brauer, R.R., 2017. Akzeptanz kooperativer Roboter im industriellen Kontext. Universitätsverlag Chemnitz, Chemnitz, 145, xxv.
- [7] D'Addona, D.M., Bracco, F., Bettoni, A., Nishino, N., Carpanzano, E., Bruzzone, A.A., 2018. Adaptive automation and human factors in manufacturing: An experimental assessment for a cognitive approach. *CIRP Annals* 67 (1), 455–458.
- [8] Taiana, M., Nascimento, C., Bernardino, A., 2013. An Improved Labelling for the INRIA Person Data Set for Pedestrian Detection, *Iberian Conference on Pattern Recognition and Image Analysis*, pp 286–295.
- [9] Cao, Z., Simon, T., Wei, S., Sheikh, Y., 2017. Realtime Multi-Person 2D Pose Estimation using Part Affinity Fields, *IEEE Conference on Computer Vision and Pattern Recognition*.
- [10] Villaseñor, L.M., Ponce, H., Espinosa-Loera, R.A., 2018. Multimodal Database for Human Activity Recognition and Fall Detection, *MPDI Proceedings 2018*, 2, 1237.
- [11] Höcherl, J., Wrede, B., Schlegl, T., 2017. Motion Analysis of Human-Human and Human-Robot Cooperation During Industrial Assembly Tasks, in: *Proceedings of the 5th International Conference on Human Agent Interaction. the 5th International Conference, Bielefeld, Germany. 17.10.2017 - 20.10.2017. ACM, New York, NY*, pp. 425–429.
- [12] Bortot, D., Ding, H., Antonopolous, A., Bengler, K., 2012. Human motion behavior while interacting with an industrial robot. *Work (Reading, Mass.)* 41 Suppl 1, 1699–1707.
- [13] Szemes, P.T., Korondi, P., Hashimoto, H., 2006. Human Walking Behavior Model for Intelligent Space, *IEEE International Conference on Mechatronics*, DOI: 10.1109/ICMECH.2006.252585
- [14] Harsch, A., Delang, K., Bdiwi, M., Breitfeld, M., P.M., 2017. Safe Human-Robot-Collaboration (HRC) based on a new concept considering human movement variability, *Vancouver*.